

Production of translationally cold barium monohalide ions

M. V. DePalatis and M. S. Chapman

School of Physics, Georgia Institute of Technology, Atlanta, Georgia 30332-0430, USA

(Received 31 May 2013; revised manuscript received 20 July 2013; published 5 August 2013)

We have produced sympathetically cooled barium monohalide ions BaX^+ ($X = \text{F}, \text{Cl}, \text{Br}$) by reacting trapped, laser-cooled Ba^+ ions with room-temperature gas-phase neutral halogen-containing molecules. Reaction rates for two of these (SF_6 and CH_3Cl) have been measured and were found to be in agreement with classical models. BaX^+ ions are promising candidates for cooling to the rovibrational ground state, and our method presents a straightforward way to produce these polar molecular ions.

DOI: [10.1103/PhysRevA.88.023403](https://doi.org/10.1103/PhysRevA.88.023403)

PACS number(s): 37.10.Rs, 37.10.Ty, 82.30.Fi, 82.20.Pm

I. INTRODUCTION

In recent years, considerable progress has been made in extending laser-cooling techniques to both neutral molecules [1–4] and molecular ions [5–8]. Cold molecular ions are of particular interest for the study of chemical reactions in the quantum regime [9], electron electric dipole moment searches [10,11], testing for time variation of fundamental constants [12], and use in cavity QED experiments [13]. Molecular ions can be prepared in low-rovibrational states in varying ways for different types of molecules. Direct optical methods have been demonstrated, for example, in MgH^+ [5] and HD^+ [6], and other ions such as N_2^+ can be prepared in the rovibrational ground state through state-selective photoionization [14]. Another promising class of molecular ions for internal cooling are alkaline-earth-metal monohalide ions, which consist of two closed-shell atomic ions. These molecules, among others, can be cooled to the rovibrational ground state via collisions with ultracold neutral atoms [15,16]. One method for producing such ions, employed in Refs. [16–18], is ablating an appropriate target. Several studies have produced other alkaline-earth-metal monohalides such as CaF^+ [19–21] via reactions with neutral molecules in the gas phase. Reactions resulting in CaF^+ ions have also been thoroughly studied theoretically [19,21], but few such efforts have been made for reactions between Ba^+ and molecules containing halogens. Ba^+ is known to react with HCl to form BaCl^+ [18], but in this case, the presence of HCl was an unintended byproduct formed by reaction of background gases and ablation products from a BaCl_2 target.

Here, we produce sympathetically, translationally cooled BaX^+ ions ($X = \text{F}, \text{Cl}, \text{Br}$) through reactions with neutral molecules at room temperature and Coulomb crystals of trapped Ba^+ ions. We determine the reaction rate constants for the production of BaF^+ and BaCl^+ , and we utilize both nondestructive motional resonance coupling and mass-selective ejection to verify the production of these molecular ions. The deduced reaction rate constants are compared with classical models and found to agree with these predictions. Producing BaX^+ ions in this way is simple and allows for the study of different barium monohalide species without significant changes in the experimental setup.

II. EXPERIMENT**A. Reaction measurements**

Experiments begin with Coulomb crystals of Ba^+ ions formed in a linear Paul trap with radius $r_0 = 3.18$ mm and rf frequency $\Omega = 2\pi \times 2.7$ MHz with the rf voltage $\varphi_+ = [U - V \cos(\Omega t)]/2$ applied to one pair of opposing electrodes and $\varphi_- = -\varphi_+$ to the other. Typical peak-to-peak rf voltages are $V = 100\text{--}400$ V for trapping (for Ba^+ , $q = 0.05\text{--}0.2$, $q = 0.12$ at $V = 240$ V) and up to ~ 1.25 kV ($q = 0.6$) during loading with $U = 0$ throughout. The barium ions are loaded by ablating a barium metal target in a similar manner as described previously [22]. Following loading, the trapping voltages are briefly adjusted to ensure that any contaminant ions of significantly different mass are ejected. Ions are confined axially with end caps separated by 25 mm. Typical end-cap voltages are $U_{\text{EC}} \approx 100\text{--}300$ V. Cooling ($\lambda = 493$ nm) and repumper ($\lambda = 650$ nm) beams are introduced axially from one end of the trap. This causes an axial sorting of barium isotopes visible as an apparent asymmetry in the Coulomb crystal structure, as shown in Fig. 1. We tune the cooling and repumper beams such that they are red detuned for maximum fluorescence of $^{138}\text{Ba}^+$ since it is the most abundant isotope and therefore maximizes the fluorescence signal. The lasers are separately stabilized to temperature-controlled cavities that are in turn locked to a 780-nm laser referenced to a Rb vapor cell (see Ref. [23] for a similar locking scheme). Data are acquired through the capture of fluorescence images obtained using a $\text{NA} = 0.34$ achromatic objective lens and an electron multiplying CCD camera (Andor iXon DV887) using exposure times of 50 ms and a total magnification of $4\times$.

In order to create and trap BaX^+ molecular ions, the reactants are leaked into the vacuum chamber at partial pressures of up to 10^{-9} torr. At these pressures, the laser-cooled ions remain in an ordered state. Each reaction measured here is of the form $\text{Ba}^+ + \text{AX} \rightarrow \text{BaX}^+ + \text{A}$ with negligible total ion loss. That is, for each reaction event, a Ba^+ ion reacts to create a trapped molecular BaX^+ ion, and so the total number of trapped ions is conserved. Measuring the rate of reaction is therefore equivalent to measuring the loss rate of Ba^+ ions. This can be seen in the structure of the Coulomb crystal as it reacts over time, as in Fig. 2, where the remaining Ba^+ ions are forced by radiation pressure in the direction of the cooling beam and heavier molecular ions form on the outside of the visible crystal structure. These

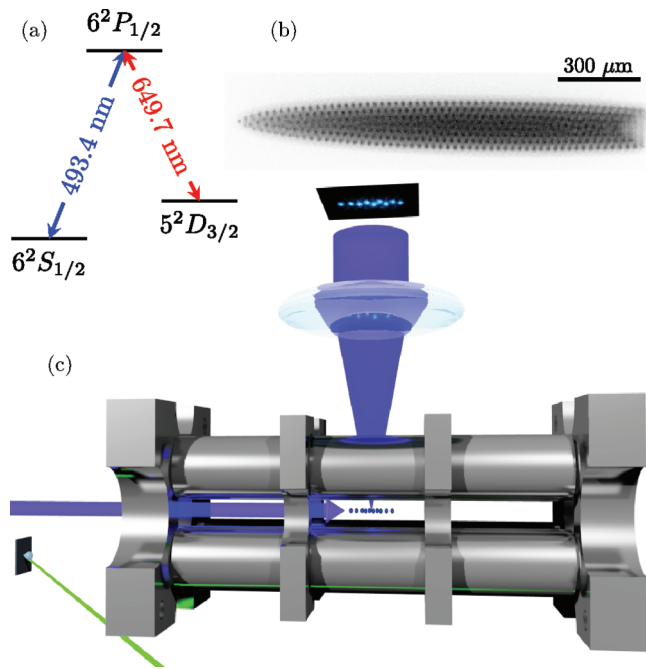


FIG. 1. (Color online) (a) Ba^+ energy levels and optical transitions. (b) A typical Coulomb crystal containing several hundred Ba^+ ions. Radiation pressure forces $^{138}\text{Ba}^+$ ions in the direction of laser propagation (to the left) and the remaining, nonfluorescing isotopes collect on the other end (right). (c) Schematic drawing of the experimental setup. Ba^+ ions are loaded via laser ablation (diagonal beam) and cooled axially (horizontal beam).

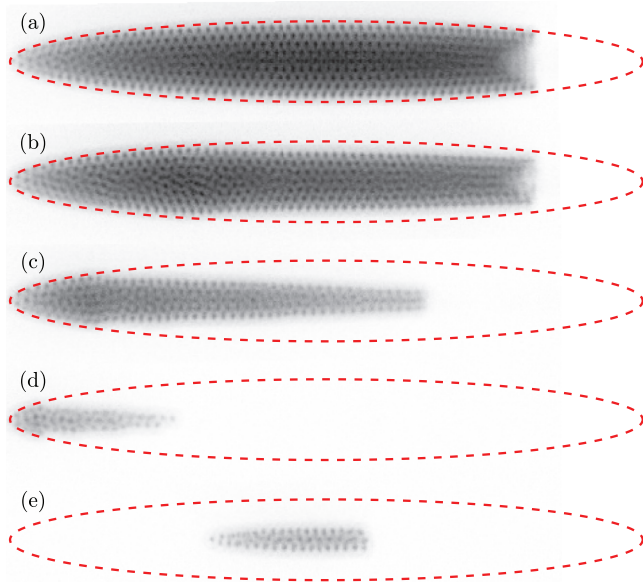


FIG. 2. (Color online) (a) A Coulomb crystal consisting of hundreds of laser-cooled $^{138}\text{Ba}^+$ ions and sympathetically cooled Ba^+ ions of other isotopes (not visible). (b)–(d) Subsequent images of the Coulomb crystal at different stages of a reaction with SF_6 . (e) The remaining Ba^+ ions as in (d) but following the ejection of heavy reaction product ions. The dashed ellipse in each image represents the approximate extent of the original Coulomb crystal in (a). Fluorescence indicates no loss of $^{138}\text{Ba}^+$ ions between (d) and (e). The major and minor diameters of each ellipse respectively measure about 1860 and 260 μm .

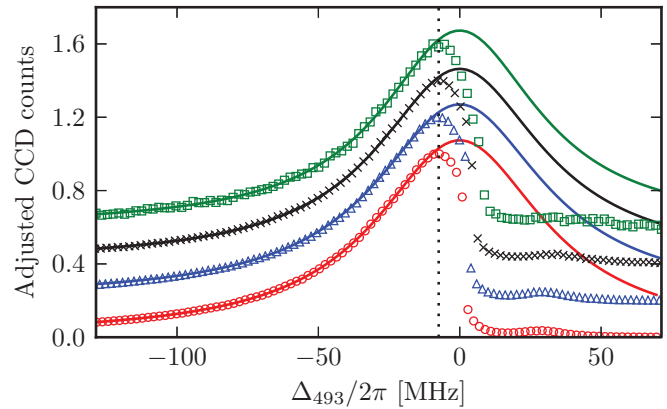


FIG. 3. (Color online) Measurements of $^{138}\text{Ba}^+$ fluorescence versus 493-nm laser detuning at different stages of the reaction with SF_6 in Fig. 2. Absolute counts are background subtracted and scaled for comparison and offset for clarity. Circles, triangles, crosses, and squares correspond respectively to Figs. 2(a)–2(d). In each case, the reaction is halted by removing the reactant gas from the chamber prior to performing the measurement. Solid lines are Lorentzian fits to the data up to the point indicated by the dotted line with an average Lorentzian linewidth of 35(1) MHz. Near the blue detuned side of resonance, fluorescence drops off dramatically as the ions are heated.

crystal structures are consistent with translationally cold, sympathetically crystallized molecular ions and are similar to those observed in related experiments which were found to be in good agreement with molecular dynamics simulations [20,24–27].

A number of methods can be used for determining the Ba^+ loss rate. The simplest is counting ions, which can be done easily for small ion crystals, or by comparing simulated images of known numbers of ions with experimental images [26]. Alternatively, the integrated fluorescence from the laser cooled ions can be measured as a function of time since the number of scattered photons is proportional to the number of ions. Although the photon scattering rate also depends on temperature, we operate the lasers in a regime where the observed fluorescence response to detuning is dominated by power broadening. By comparing this response for Coulomb crystals at different stages of a reaction, we find no significant change to the measured line shapes, and thus the scattering rate per ion can be treated as constant for a fixed detuning (see Fig. 3). Other experiments performed under similar conditions have also found that measuring the laser-cooled ion loss rate using fluorescence is in good agreement with other ion-counting methods [25,26]. A representative Ba^+ loss rate measurement using Ba^+ fluorescence over time is shown in Fig. 4. The good agreement with an exponential decay further supports the use of fluorescence as a measure of the number of laser-cooled ions.

Reaction rate constants can be determined by measuring Ba^+ loss rates at different pressures and extracting the slope of a linear fit to these data. We utilize SF_6 , CH_3Cl , and Br_2 as reactants. SF_6 and CH_3Cl are in the gas phase at room temperature and are stored in a reservoir of about 500 mL at pressures of slightly more than 1 atm which is connected to the inlet of the leak valve. Bromine is a liquid at room temperature, but has a sufficiently high vapor pressure of Br_2

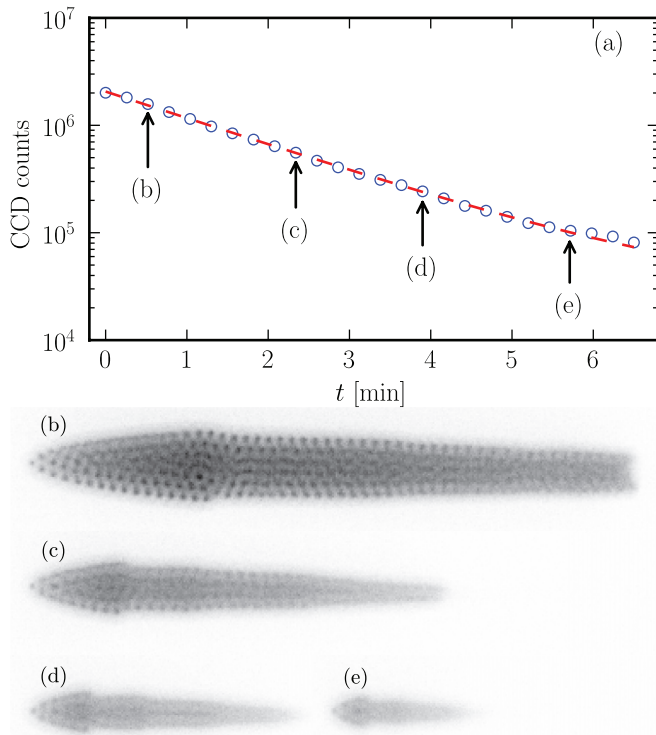


FIG. 4. (Color online) (a) Ba^+ loss rate measurement in the presence of SF_6 at a partial pressure of 2.8×10^{-10} torr using total fluorescence. The dashed line is a nonlinear least-squares fit to an exponential decay. (b)–(e) Snapshots of the Coulomb crystal at each point indicated in (a).

(~ 185 torr [28]) to use as a gas-phase reactant. A few mL of liquid bromine are added to a small reservoir at rough vacuum which is connected to the leak-valve inlet.

B. Mass determination

In order to analyze reaction products, it is necessary to determine the masses of trapped ions following reactions. One common nondestructive method is to excite motional resonances of the trapped ions by applying an additional ac voltage to the trap electrodes. Ions are heated when in motional resonance with this applied voltage, which results in a significant increase of temperature for all trapped ions through their mutual Coulomb repulsion. This increased temperature changes the laser-cooled ion fluorescence and thus can be used to determine relative masses of sympathetically cooled ions [24,29,30]. For a single ion, axial and radial frequencies are given, respectively, by $\omega_z = (2Ze\kappa U_{\text{EC}}/mz_0^2)^{1/2}$ and $\omega_r = (\omega_0^2 - \omega_z^2/2)^{1/2}$, where $\omega_0 = ZeV/\sqrt{2}mr_0^2\Omega$, κ is a unitless geometric constant, and z_0 is half the distance between the end caps. However, cotrapping ion crystals of different species is well known to introduce shifts away from these single-ion frequencies, which complicates attempts to use the motional resonance frequencies to precisely determine the masses of the trap contents [31]. Furthermore, the preceding expressions are derived assuming the trapping pseudopotential is quadratic in each dimension. This is generally a good approximation in the radial direction, but due to the geometry of our trap, the axial potential deviates from a quadratic

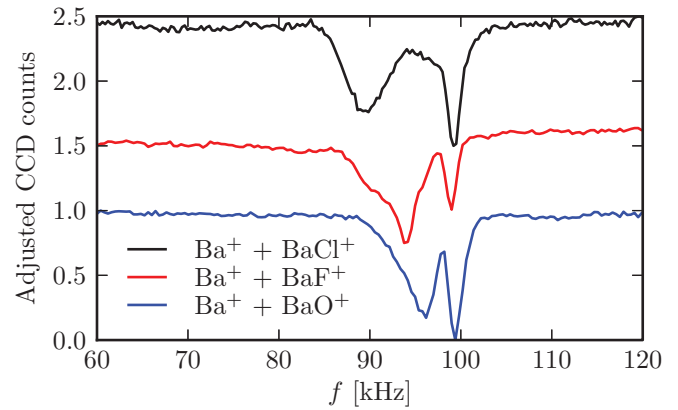


FIG. 5. (Color online) Comparison of ac frequency sweeps after Ba^+ ions react with (top) CH_3Cl , (middle) SF_6 , and (bottom) O_2 . CCD counts are scaled and offset for clarity. In each case, the broader resonance at lower frequencies is due to the heavier sympathetically cooled product ions while the narrower resonance at higher frequencies is due to the laser-cooled Ba^+ ions.

approximation significantly for large Coulomb crystals. For these reasons, we do not use ac frequency sweeps to absolutely identify sympathetically cooled ion masses, but rather to compare results following different reactions in order to deduce likely products. We drive radial modes by applying an ac voltage of up to several hundred mV to one of the four rf electrodes. Typical results from frequency sweeps of Coulomb crystals composed of Ba^+ and reaction products are presented in Fig. 5.

An alternative, destructive method utilizes the Mathieu stability parameters $q = 2ZeV/mr_0^2\Omega^2$ and $a = 4ZeU/mr_0^2\Omega^2$. By applying dc offset voltages $\pm U/2$ to each rf electrode, a portion of the q - a stability boundary for heavy, sympathetically cooled A^+ ions can be determined by watching for a change in the crystal structure and a contraction of the crystal, which appears as an overall shift of the fluorescing ions toward the center of the trap. These changes in the crystal indicate the ejection of the heavier ions, thereby allowing for determination of their mass. Ba^+ ions are first loaded into the trap, then allowed to react with a reactant gas for several seconds until the crystal structure clearly indicates the presence of heavier sympathetically cooled ions. The rf voltage is then brought to a particular value of V and dc offsets are pulsed with increasing voltage until the crystal structure changes and shifts towards the center of the trap, indicating the ejection of A^+ ions. This value of U is recorded and the dc voltage is increased further in order to find the value of U at which Ba^+ is ejected. Overlaying these U , V pairs on top of the theoretical stability boundaries then gives us a more precise determination of the product masses than do ac frequency sweeps. Because the probe for measuring rf voltage is not well calibrated, the probe reading is multiplied by a scaling factor which is chosen by fitting the U , V pairs for Ba^+ to its theoretical stability boundary. In order to test this method, we first performed these measurements on Coulomb crystals consisting of Ba^+ and BaO^+ formed by leaking O_2 into the chamber. This utilizes the endothermic reaction $\text{Ba}^+ + \text{O}_2 \rightarrow \text{BaO}^+ + \text{O}$, which

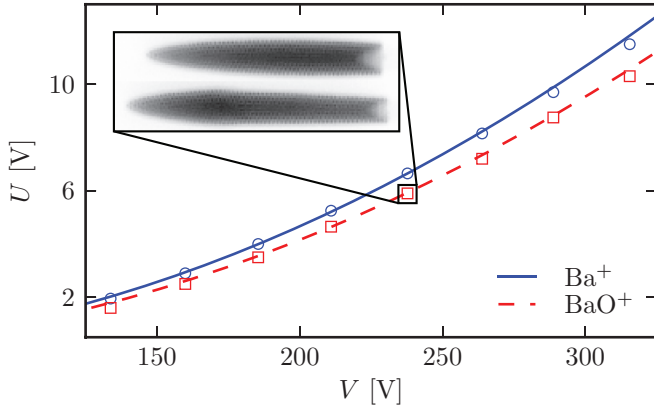


FIG. 6. (Color online) Destructive mass determination following reactions between Ba^+ and O_2 . Squares (circles) indicate voltages for ejection of sympathetically cooled molecular ions (laser-cooled Ba^+ ions) and curves represent the theoretical stability region boundaries. The inset images show crystals before (bottom) and after (top) ejecting BaO^+ ions at the point indicated.

has been studied extensively elsewhere [26,32]. The results of these measurements are illustrated in Fig. 6.

III. CHEMICAL REACTIONS

The simplest model for characterizing the rate of reactions between ions and neutral, nonpolar molecules is the Langevin model [33]. Assuming spherical symmetry and given the charge Ze on the ion and polarizability α of the neutral molecule, the Langevin reaction rate constant can be expressed in Gaussian-cgs units as

$$k_L = 2\pi Ze \sqrt{\frac{\alpha}{\mu}}, \quad (1)$$

where μ is the reduced mass. Typical rates calculated from this model are of order $10^{-9} \text{ cm}^3 \text{ s}^{-1}$. The Langevin model is not comprehensive, but nevertheless serves as a useful estimate of reaction rates and many nonpolar molecules do indeed react at or near the predicted rate. For polar molecules, the Langevin rate must be corrected by taking into account the dipole moment d . The corrected rate constant is expressed as [34]

$$k_c = k_L + ck_D = 2\pi Ze \left(\sqrt{\frac{\alpha}{\mu}} + cd \sqrt{\frac{2}{\pi \mu k_B T}} \right), \quad (2)$$

where $0 < c < 1$ and k_D is the component of the rate constant associated with a “locked in” dipole. There are several methods for estimating c including the average dipole orientation theory [35], but to lowest order, by setting $c = 1$, Eq. (2) can be used to estimate an upper bound on the reaction rate.

In order to translate Ba^+ loss rate measurements into a reaction rate constant, we repeat these measurements at several different reactant gas pressures. The measured reaction rate constant k is then the slope of a linear fit to the Ba^+ loss rate versus pressure data. We use a Varian UHV-24 ion gauge to measure pressures and apply appropriate correction factors ϵ in order to obtain a reading more suitable for the reactant introduced. This gives us corrected rate constants $k_\epsilon = \epsilon k$. Ultimately, since the ion gauge was not calibrated, the

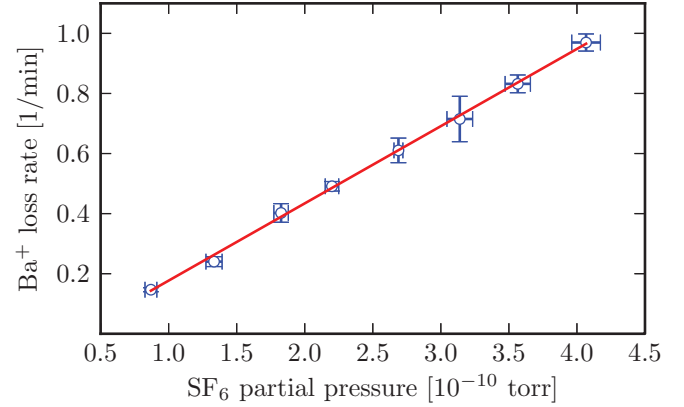
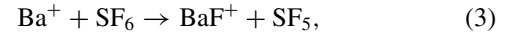


FIG. 7. (Color online) $\text{Ba}^+ + \text{SF}_6$ reaction rate measurements. Each point represents the average measured Ba^+ loss rate at a given target partial pressure. Vertical error bars represent the standard deviation of the measured Ba^+ loss rates and horizontal error bars indicate the standard deviation of the pressure recorded by the ion gauge for each measurement. The solid line is a linear fit to the data. Partial pressures are corrected using the ion-gauge correction factor $\epsilon = 2.3$.

dominant source of error lies with the pressure measurements and thus the measured values k_ϵ are accurate only within a factor of 2 or 3.

A. Sulfur hexafluoride

To form BaF^+ ($q = 0.10$ at $V = 240 \text{ V}$), we utilize SF_6 . The expected reaction is



which from known thermochemistry is exothermic by 2.8 eV [28]. In order to determine the reaction rate constant k between Ba^+ and SF_6 , a series of measurements of the Ba^+ loss rate were made at several different partial pressures of SF_6 . A linear fit of the measured Ba^+ loss rates versus partial pressure then yields the reaction constant (see Fig. 7), which is listed in Table I. We find that the reaction between Ba^+ and SF_6 proceeds consistent with the Langevin model.

Energy considerations imply that Eq. (3) should be the dominant reaction between Ba^+ and SF_6 , but to verify this,

TABLE I. Reaction rate constants between Ba^+ and neutral reactants used in this work in units of $10^{-9} \text{ cm}^3 \text{ s}^{-1}$. Reaction rate constants k using uncorrected ion-gauge pressure readings are multiplied by ion-gauge correction factors ϵ to obtain the corrected reaction rate constants $k_\epsilon = \epsilon k$. Ion-gauge correction factors are obtained from Ref. [36]. Also listed are the theoretical Langevin rate constant (k_L), dipole correction term (k_D), and upper bound corrected Langevin rate constant ($k_c \leq k_L + k_D$) using polarizabilities from Refs. [37–40] and dipole moment from Ref. [41].

Reactant	k	ϵ	k_ϵ	k_L	k_D	k_c
SF_6	0.6	2.3	1.3	0.6	–	–
CH_3Cl	0.6	2.6	1.6	0.8	2.0	≤ 3.7
Br_2	–	3.8	–	0.7	–	–
I_2	–	5.4	–	0.8	–	–

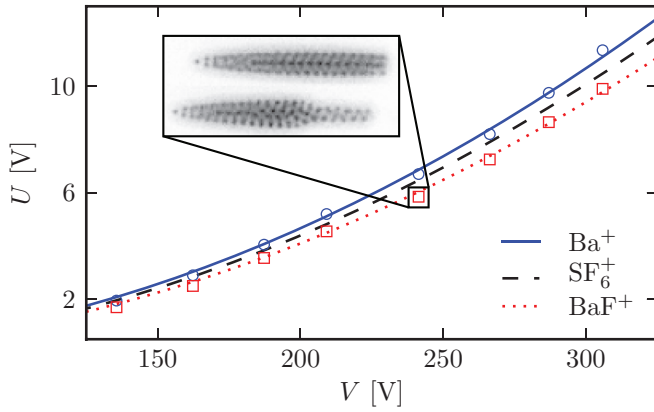


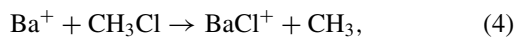
FIG. 8. (Color online) Mass determination following reactions between Ba^+ and SF_6 . The inset images show crystals before (bottom) and after (top) ejection of BaF^+ at the point indicated. The curves represent theoretical stability region boundaries.

we performed mass spectroscopic measurements on reaction products. It should be noted that the mass of BaF^+ (≈ 157 amu) is near the mass of SF_6^+ (≈ 146 amu). Given the known frequency shift effects and fairly low mass resolution, frequency sweeps alone are not sufficient to preclude the possibility that the reaction between Ba^+ and SF_6 is simple charge exchange. However, the ionization energy of SF_6 is known to be >15 eV compared to 5.2 eV for Ba [42,43], making such a reaction energetically unfavorable. Furthermore, SF_6^+ is expected to rapidly decay into SF_5^+ , which is lighter than $^{138}\text{Ba}^+$ by more than 10 amu [44]. Lighter sympathetically cooled ions are more tightly confined at a given rf voltage, and therefore form a light core at the center of the Coulomb crystal. Likewise, heavier sympathetically cooled ions form shells on the exterior of the Coulomb crystal. Since we only observe the latter crystal structures, we conclude that all reaction products are heavier than Ba^+ .

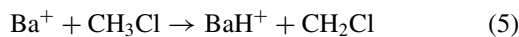
To further rule out the possibility of charge exchange between Ba^+ and SF_6 , we performed destructive mass determination measurements as outlined in Sec. II B on Coulomb crystals after reacting with SF_6 . The results of these measurements following both reactions $\text{Ba}^+ + \text{O}_2$ and $\text{Ba}^+ + \text{SF}_6$ are shown in Fig. 8. Given these results and the previously discussed energy considerations, we conclude that we are, in fact, producing BaF^+ by the reaction Eq. (3).

B. Methyl chloride

For the production of BaCl^+ ($q = 0.09$ at $V = 240$ V), Ba^+ ions were allowed to react with CH_3Cl via the reaction



which is exothermic by 0.6 eV [28]. The reaction



is estimated to be endothermic by 2.3 eV with respect to the ground state of Ba^+ , but becomes exothermic by 0.2 eV for Ba^+ ions in the $6^2P_{1/2}$ excited state [28]. This implies that there could be some amount of BaH^+ produced when measuring Ba^+ loss rates in the presence of CH_3Cl . However, the lower motional resonance frequency in Fig. 5 indicates

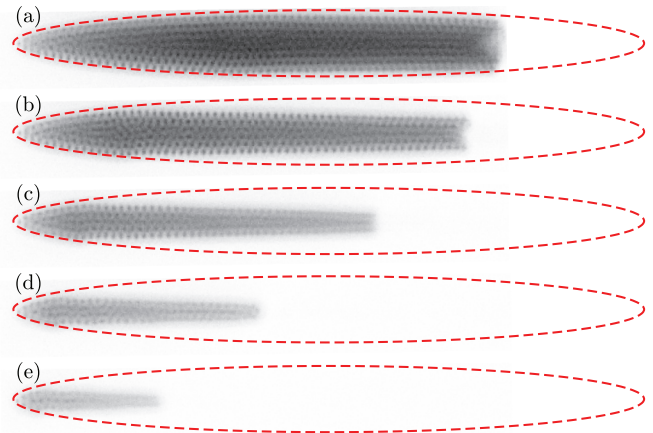


FIG. 9. (Color online) Ba^+ ions undergoing a reaction in the presence of $<10^{-10}$ torr of CH_3Cl at times (a) $t = 0$, (b) $t = 180$ s, (c) $t = 435$ s, (d) $t = 705$ s, and (e) $t = 1050$ s. Reactions have already begun in (a) prior to data acquisition, which can be seen in the slight deformation of the ion crystal exterior near the center. The red ellipses indicate the approximate extent of the initial crystal prior to reaction and have major and minor diameters of approximately 2080 and 220 μm , respectively.

the production of BaCl^+ , and given that observed Coulomb crystals take on the expected shape for significantly heavier sympathetically cooled ions (see Fig. 9) and that reaction (5) is endothermic with the ground and metastable states of Ba^+ , we expect that reaction (4) is the dominant reaction [45]. Assuming this to be the case, the reaction rate constant was measured in the same manner as described above for reactions with SF_6 . The results of these measurements are shown in Fig. 10 and the associated rate constant compared with theory is listed in Table I. Future studies with improved mass resolution via time-of-flight mass spectrometry [18] or high-precision nondestructive techniques [46] will be necessary to fully analyze the reaction pathways and measure branching ratios for all possible reactions between Ba^+ and CH_3Cl .

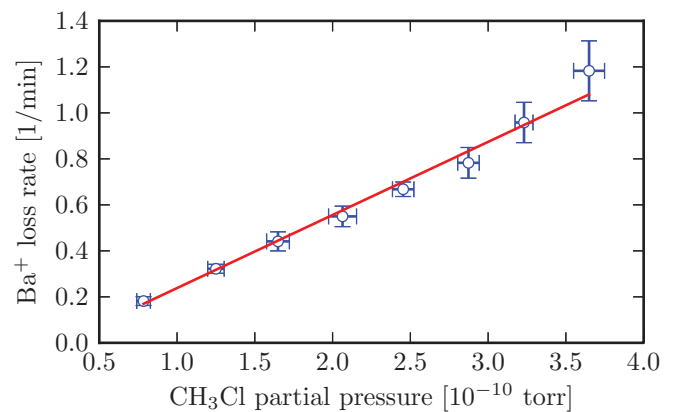


FIG. 10. (Color online) $\text{Ba}^+ + \text{CH}_3\text{Cl}$ reaction rate measurements. Partial pressures are corrected using the ion-gauge correction factor $\epsilon = 2.6$.

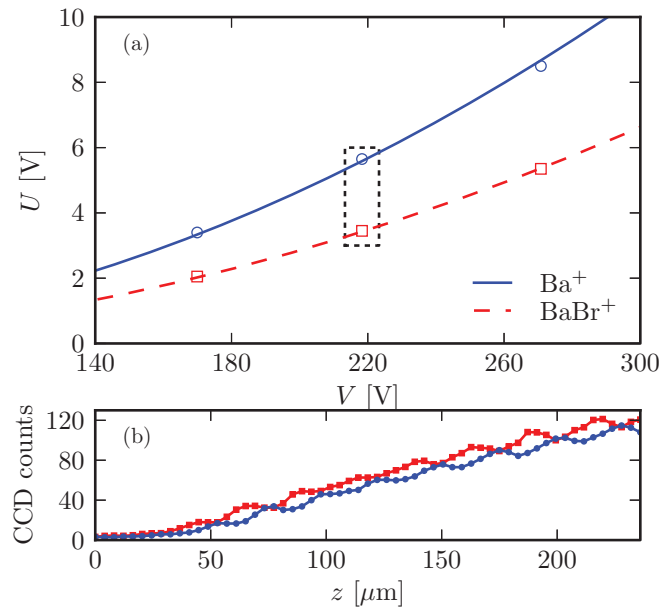
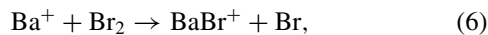


FIG. 11. (Color online) (a) Destructive mass determination following reactions between Ba^+ and Br_2 . (b) Integrated CCD counts along the center and near one end of the Coulomb crystals indicated with the dotted box in (a) both before (curve with squares) and after (curve with circles) applying a U pulse to eject BaBr^+ ions. The shift to the right indicates the successful ejection of heavy ions.

C. Bromine and iodine

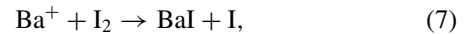
BaBr^+ ($q = 0.07$ at $V = 240$ V) is produced through the reaction



which is exothermic by about 2.2 eV [28]. In order to get enough Br_2 in the vicinity of the trapped Ba^+ ions, it was necessary to increase the leak rate considerably compared to what was required for SF_6 and CH_3Cl . This allowed other contaminants such as O_2 , CO_2 , and H_2O into the chamber simultaneously, which also react with Ba^+ . However, reactions between Ba^+ and both O_2 and CO_2 are endothermic with the ground state [26], and the last is barely exothermic [32]. Thus, by blocking the cooling beams, primarily BaBr^+ is produced. Measuring Ba^+ loss rates was not possible because of this, but

it appeared to be much slower than with the other reactants. We suspect this was, in part, due to the liquid nature of Br_2 at room temperature combined with the fact that there was no direct line of sight between the leak valve and the trapped ions. Due to the slow apparent Ba^+ loss rate, producing enough BaBr^+ to obtain a good ac frequency sweep mass spectrum was not practical, so destructive measurements as in Fig. 8 were performed and are shown in Fig. 11. Because the number of product ions was very small compared to the number of Ba^+ ions, ejection of reactants is noted by watching for a shift in the outermost ion towards the center rather than watching for a large change in crystal structure.

We also attempted to produce BaI^+ ($q = 0.06$ at $V = 240$ V) in a similar manner using the reaction



which is also exothermic by about 2.2 eV. I_2 is a solid at room temperature with a vapor pressure of around 300 mtorr. A sample of a few grams of I_2 was placed in a small reservoir evacuated to rough vacuum before being connected to the leak valve inlet. No BaI^+ production was observed, presumably for similar reasons as mentioned above. Future studies with a more optimal chamber geometry could allow for study of reaction (7) at room temperature.

IV. CONCLUSION

In summary, we have demonstrated a simple method for the production of translationally cold BaF^+ , BaCl^+ , and BaBr^+ by reacting Ba^+ ions with SF_6 , CH_3Cl , and Br_2 . Reaction rate constants between Ba^+ and SF_6 and CH_3Cl were measured and found to be consistent with classical predictions within the limitations of pressure measurements. With some changes to the vacuum chamber, similar rate constant measurements could be made for the reactions of Ba^+ with I_2 and Br_2 .

ACKNOWLEDGMENTS

We thank Michael Schatz's laboratory for the use of SF_6 . We also gratefully acknowledge useful discussions with Richard Darst, James Goeders, Ncamiso Khanyile, and Ken Brown. This work was supported by the National Science Foundation and the Office of Naval Research.

-
- [1] E. S. Shuman, J. F. Barry, and D. DeMille, *Nature (London)* **467**, 820 (2010).
 [2] I. Manai, R. Horchani, H. Lignier, P. Pillet, D. Comparat, A. Fioretti, and M. Allegrini, *Phys. Rev. Lett.* **109**, 183001 (2012).
 [3] B. K. Stuhl, M. T. Hummon, M. Yeo, G. Qumner, J. L. Bohn, and J. Ye, *Nature (London)* **492**, 396 (2012).
 [4] M. T. Hummon, M. Yeo, B. K. Stuhl, A. L. Collopy, Y. Xia, and J. Ye, *Phys. Rev. Lett.* **110**, 143001 (2013).
 [5] P. F. Staunum, K. Hjbjerre, P. S. Skyt, A. K. Hansen, and M. Drewsen, *Nat. Phys.* **6**, 271 (2010).
 [6] T. Schneider, B. Roth, H. Duncker, I. Ernsting, and S. Schiller, *Nat. Phys.* **6**, 275 (2010).
 [7] J. H. V. Nguyen, C. R. Viteri, E. G. Hohenstein, C. D. Sherrill, K. R. Brown, and B. Odom, *New J. Phys.* **13**, 063023 (2011).
 [8] U. Bressel, A. Borodin, J. Shen, M. Hansen, I. Ernsting, and S. Schiller, *Phys. Rev. Lett.* **108**, 183003 (2012).
 [9] S. Willitsch, M. T. Bell, A. D. Gingell, and T. P. Softley, *Phys. Chem. Chem. Phys.* **10**, 7200 (2008).
 [10] E. R. Meyer and J. L. Bohn, *Phys. Rev. A* **78**, 010502 (2008).
 [11] K. C. Cossel, D. N. Gresh, L. C. Sinclair, T. Coffey, L. V. Skripnikov, A. N. Petrov, N. S. Mosyagin, A. V. Titov, R. W. Field, E. R. Meyer *et al.*, *Chem. Phys. Lett.* **546**, 1 (2012).
 [12] V. V. Flambaum and M. G. Kozlov, *Phys. Rev. Lett.* **99**, 150801 (2007).

- [13] D. I. Schuster, L. S. Bishop, I. L. Chuang, D. DeMille, and R. J. Schoelkopf, *Phys. Rev. A* **83**, 012311 (2011).
- [14] X. Tong, A. H. Winney, and S. Willitsch, *Phys. Rev. Lett.* **105**, 143001 (2010).
- [15] E. R. Hudson, *Phys. Rev. A* **79**, 032716 (2009).
- [16] W. G. Rellergert, S. T. Sullivan, S. J. Schowalter, S. Kotochigova, K. Chen, and E. R. Hudson, *Nature (London)* **495**, 490 (2013).
- [17] K. Chen, S. J. Schowalter, S. Kotochigova, A. Petrov, W. G. Rellergert, S. T. Sullivan, and E. R. Hudson, *Phys. Rev. A* **83**, 030501 (2011).
- [18] S. J. Schowalter, K. Chen, W. G. Rellergert, S. T. Sullivan, and E. R. Hudson, *Rev. Sci. Instrum.* **83**, 043103 (2012).
- [19] J. N. Harvey, D. Schröder, W. Koch, D. Danovich, S. Shaik, and H. Schwarz, *Chem. Phys. Lett.* **273**, 164 (1997).
- [20] S. Willitsch, M. T. Bell, A. D. Gingell, S. R. Procter, and T. P. Softley, *Phys. Rev. Lett.* **100**, 043203 (2008).
- [21] A. D. Gingell, M. T. Bell, J. M. Oldham, T. P. Softley, and J. N. Harvey, *J. Chem. Phys.* **133**, 194302 (2010).
- [22] L. R. Churchill, M. V. DePalatis, and M. S. Chapman, *Phys. Rev. A* **83**, 012710 (2011).
- [23] F. Rohde, M. Almendros, C. Schuck, J. Huwer, M. Hennrich, and J. Eschner, *J. Phys. B: At., Mol. Opt. Phys.* **43**, 115401 (2010).
- [24] B. Roth, A. Ostendorf, H. Wenz, and S. Schiller, *J. Phys. B: At., Mol. Opt. Phys.* **38**, 3673 (2005).
- [25] B. Roth, P. Blythe, H. Wenz, H. Daerr, and S. Schiller, *Phys. Rev. A* **73**, 042712 (2006).
- [26] B. Roth, D. Offenberger, C. B. Zhang, and S. Schiller, *Phys. Rev. A* **78**, 042709 (2008).
- [27] N. Kimura, K. Okada, T. Takayanagi, M. Wada, S. Ohtani, and H. A. Schuessler, *Phys. Rev. A* **83**, 033422 (2011).
- [28] D. R. Lide, *CRC Handbook of Chemistry and Physics*, 88th ed. (CRC Press, Boca Raton, FL, 2007).
- [29] B. Roth, P. Blythe, and S. Schiller, *Phys. Rev. A* **75**, 023402 (2007).
- [30] H. Landa, M. Drewsen, B. Reznik, and A. Retzker, *New J. Phys.* **14**, 093023 (2012).
- [31] T. Baba and I. Waki, *J. Appl. Phys.* **92**, 4109 (2002).
- [32] E. Murad, *J. Chem. Phys.* **77**, 2057 (1982).
- [33] G. Gioumousis and D. P. Stevenson, *J. Chem. Phys.* **29**, 294 (1958).
- [34] J. Troe, *Chem. Phys. Lett.* **122**, 425 (1985).
- [35] T. Su and M. T. Bowers, *J. Chem. Phys.* **58**, 3027 (1973).
- [36] *UHV-24/UHV-24p Ionization Gauge Instruction Manual* (Agilent Technologies, Lexington, MA, 2004), Revision E.
- [37] Z. Karpas and Z. Berant, *J. Phys. Chem.* **93**, 3021 (1989).
- [38] T. N. Olney, N. Cann, G. Cooper, and C. Brion, *Chem. Phys.* **223**, 59 (1997).
- [39] G. Maroulis, C. Makris, U. Hohm, and D. Goebel, *J. Phys. Chem. A* **101**, 953 (1997).
- [40] G. Maroulis and C. Makris, *Mol. Phys.* **91**, 333 (1997).
- [41] R. D. Johnson (editor), *NIST Computational Chemistry Comparison and Benchmark Database* (National Institute of Standards and Technology, Gaithersburg, MD, 2011), Release 15b; <http://cccbdb.nist.gov/>.
- [42] S. G. Lias, in *NIST Chemistry WebBook*, edited by P. J. Linstrom and W. G. Mallard (National Institute of Standards and Technology, Gaithersburg MD, 2011); <http://webbook.nist.gov>.
- [43] H. Karlsson and U. Litzn, *Phys. Scr.* **60**, 321 (1999).
- [44] H. Tachikawa, *J. Phys. B: At., Mol. Opt. Phys.* **33**, 1725 (2000).
- [45] We were unable to locate sufficient data in the literature to estimate the reaction enthalpy for the reaction $\text{Ba}^+ + \text{CH}_3\text{Cl} \rightarrow \text{BaCH}_3^+ + \text{Cl}$ and therefore determine whether it would be energetically allowable. However, it is sufficiently heavier than Ba^+ to be resolvable with ac frequency sweeps. Since no such resonances were observed, this reaction can be ruled out.
- [46] M. Drewsen, A. Mortensen, R. Martinussen, P. Staunum, and J. L. Sørensen, *Phys. Rev. Lett.* **93**, 243201 (2004).